A new method to compute periodic orbits in general symplectic maps

Preprint · March 2020

CITATIONS
0

READS
38

4 authors, including:

Renato Calleja
Universidad Nacional Autónoma de México
34 PUBLICATIONS **373** CITATIONS
SEE PROFILE

Diego del-Castillo-Negrete
Oak Ridge National Laboratory
150 PUBLICATIONS **2,833** CITATIONS
SEE PROFILE

David Martinez-del-Rio
Universidad Nacional Autónoma de México
3 PUBLICATIONS **4** CITATIONS
SEE PROFILE

A new method to compute periodic orbits in general symplectic maps

R. Calleja*†, D. del-Castillo-Negrete⋆‡, D. Martínez-del-Río*†,††A. Olvera*‡‡

* IIMAS-UNAM, Mexico City, Mexico 04510

⋆ Oak Ridge National Laboratory, Oak Ridge, Tennessee 37831-8071

Abstract

The search of high-order periodic orbits has been typically restricted to problems with symmetries that help to reduce the dimension of the search space. Well-known examples include reversible maps with symmetry lines. The present work proposes a new method to compute high-order periodic orbits in twist maps without the use of symmetries. The method is a combination of the parameterization method in Fourier space and a Newton-Gauss multiple shooting scheme. The parameterization method has been successfully used in the past to compute quasi-periodic invariant circles. However, this is the first time that this method is used in the context of periodic orbits. Numerical examples are presented showing the accuracy and efficiency of the proposed method. The method is also applied to verify the renormalization prediction of the residues' convergence at criticality (extensively studied in reversible maps) in the relatively unexplored case of maps without symmetries.

1 Introduction

The systematic study of dynamical systems with low number degrees of freedom started at the beginning of last century with the discovery of heteroclinic phenomena in periodic orbits. Poincaré and Birkhoff studied in detail the existence of periodic orbits in discrete dynamical systems, in particular twist maps that preserve area. The existence and uniformity

†calleja@mym.iimas.unam.mx

‡delcastillod@ornl.gov

††dmr@mym.iimas.unam.mx

‡‡aoc@mym.iimas.unam.mx

of these periodic orbits with respect to their rotation number allowed its use as a tool to analyze other invariant objects that persist in almost integrable twist maps. From the results obtained by Birkhoff [1] it was possible to implement a procedure to approximate invariant tori and determine their properties. Later on, with the arrival of digital computers it was possible to implement search algorithms for these invariant objects through periodic orbits of rotation numbers that approximate the invariant object. Studies from the 60's and 70's, including Chirikov [2], Greene [3], Kadanoff [4] and others obtained interesting results relying on numerical experiments performed on increasingly powerful computers.

The Greene's residue criterion, arguably the most accurate and most used method to determine the persistence or destruction of invariant circles, relies on finding high order periodic orbits for critical parameter values.

As a result from these studies, the renormalization theory of twist maps was introduced [5] and it was possible to show the universal behavior of several dynamical phenomena when the parameters are close to the destruction of invariant curves [4, 6]. All these results were obtained with the help of periodic orbits. As the numerical capabilities increased, the numerical experiments on periodic orbits were performed on higher order periods, reaching order of tens of millions limited only by the used arithmetic precision. In this way it was possible to study the scenarios predicted by the renormalization theory and to verify numerically the results of Aubry-Mather theory.

Nevertheless, the numerical study of periodic orbits in area preserving twist maps (APTM's) has been mostly limited to a particular kind of maps known as *reversible maps*. The fundamental property of these maps is that it is possible to write them as the composition of two involutions, maps with the property that their composition with themselves is the identity. The involutions invariant sets are usually one-dimensional sets, referred as symmetry lines. Using the theory of DeVogelaere [7, 3] it can be proved that two iterates of every periodic orbit lay in these invariant sets. This result allows to simplify the search of periodic orbits with the use of one-dimensional methods (1D-quasi-Newton methods). The good behavior of these methods allows to compute periodic orbits of very high order ($\sim 10^7$) and for which the limit on the order depends only on the machine precision used. For this reason, only in reversible maps has been possible to study dynamical phenomena in detail. However the number and kind of twist maps that are reversible is limited, the most famous of these maps is the standard map introduced by Chirikov and Taylor [1, 2, 8, 9]. Non-twist reversible maps have been also extensively studied, for example Refs. [10, 11, 12, 13, 14, 15]. Unfortunately many dynamical systems that can be reduced to APTM's can not be studied in the same way as reversible maps either because the lack of knowledge or the actual impossibility of writing them as reversible maps. In this case, the search must be done in two or more dimensions and, as it is well known, Newton methods in two or higher dimensions may have fractal basin of attraction. This same problem has been observed in the study of symplectic maps in $\mathbb{R}^4$,

as in the case of Froeschlé map [16, 17]. In these cases, the computation of periodic orbits is limited to relatively lower order periods.

This work presents a new procedure to find numerically periodic orbits of general area preserving maps without the use of symmetries. The metodology is based on the implementation of the parameterization method developed by de la Llave and Calleja [18, 19] based in Ref. [20] (see also Ref. [21]), that allows to approximate continuous invariant objects like invariant circles when applied on two-dimensional maps. This implementation of the method is based on the computation of Fourier modes of an invariant object of fixed rotation number and allows to give lower bounds to the critical values of the parameters for which the invariant object exist as a continuous set.

The proposed method consists of two steps. First, a modified version of the parameterization method to obtain a suitable seed, and second, a Newton-Gauss method to refine the result. This scheme allows to compute periodic orbits of high periods ($\sim O(10^7)$). As it will be explained in Sec. 3, because of the use of the parameterization method, the periodic orbits that we look for are monotone and approximate invariant circles.

The authors found the necessity to develop a new method to compute periodic orbits when studying the self-consistent transport phenomena in a reduced plasma physic model that consisted in a large number of standard-like maps coupled by a mean field [22, 23]. The study of the global stability of the model lead to computation of the invariant curves that can be approximated by periodic orbits of high order period in non autonomous maps.

The present work is organized as follows. Section 2 presents some the classic notation and definitions used. Section 3 contains a short introduction of the standard parameterization method introduced by de la Llave et al. [20, 24]. Section 4 presents our new method for computation of periodic orbits and describe how the different parts of the method solve the problems that arise. Section 5 presents different tests we performed to understand the behavior and reaches of each part of the method and verify the consistency with the theory. In section 6 we present different test results over the periodic orbits data obtained by the full compound method to verify different renormalization theory predictions for twist maps and, in Section 7 we present a discussion of these results and conclusions about the efficiency and possible future applications of our new method.

2 Preliminaries

The maps of interest in the present work are symplectic diffeomorphisms on the cylinder, $T : \mathbb{S} \times \mathbb{R} \to \mathbb{S} \times \mathbb{R}$. For sake of brevity, the reader is referred to Refs. [1, 25, 26] for the standard definitions. A periodic orbit with rotation number p/q on the lift of map T,

$\tilde{T} : \mathbb{R}^2 \to \mathbb{R}^2$, satisfies the relation,

$$\tilde{T}^q(z_0) = z_0 + P\,, \qquad \text{where} \;\; z_0 \in \mathbb{R}^2,\; P = \begin{pmatrix} p \\ 0 \end{pmatrix}\,. \tag{1}$$

A map T is called *reversible* [27, 28, 16] if it can be written as the composition, $T = I_2 \circ I_1$, of two functions I_1 and I_2 with the property,

$$I_k \circ I_k = Id\,, \qquad k = 1, 2\,, \tag{2}$$

where Id is the identity. Functions that fulfill this property are called *involutions*. A list of properties of reversible maps can be found in Ref. [29] and further properties of involutions in Refs. [30, 31].

The invariant sets of involutions are called symmetry lines[1]. It can be proved (see Refs. [25, 6, 30]) that for any monotone periodic orbit of a reversible map with rotation number $\omega = p/q$, at least two points of the orbit lay on the symmetry lines.

The existence of symmetry lines allows to reduce the search of periodic orbits of a reversible twist map [3, 32] and non twist map [12] from a 2-D problem to a 1-D search on the symmetry line. In 1-D there are plenty of methods to search for zeros of a equation and in particular the quasi-Newton methods are efficient and well behaved [33]. This is why it is possible to find periodic orbits of high order period, $q \sim 10^6 - 10^7$. The only limit for their computation is the machine precision and not the complexity of the perturbation function presented, as it can be appreciated in Ref. [32] for different (reversible) maps.

The most common example of the use of symmetry lines to find periodic orbits is the case of the *standard map* defined as,

$$\mathcal{S}_\kappa \begin{pmatrix} x \\ y \end{pmatrix} = \begin{pmatrix} x + y - V'(x) \\ y - V'(x) \end{pmatrix}\,, \tag{3}$$

with the perturbation function $V'(x)$,

$$V'(x) = \frac{\kappa}{2\pi} \sin(2\pi x)\,. \tag{4}$$

This particular version of the standard map, allows a decomposition in two involutions I_1 and I_2, $\mathcal{S}_\kappa = I_2 \circ I_1$, defined as,

$$I_1 \begin{pmatrix} x \\ y \end{pmatrix} = \begin{pmatrix} -x \\ y - \frac{\kappa}{2\pi} \sin(2\pi x) \end{pmatrix}\,, \qquad I_2 \begin{pmatrix} x \\ y \end{pmatrix} = \begin{pmatrix} y - x \\ y \end{pmatrix}\,. \tag{5}$$

[1] In Ref. [30] a more general definition is used for symmetry lines.

Considering that x is an angular variable ($x \in [0, 1)$), the symmetry lines for I_1 are: $x = 0$ and $x = 1/2$, and for I_2: $x = \frac{y}{2}$ and $x = \frac{y+1}{2}$, which can be appreciated in Fig. 1 superposed over the phase space of standard map for $\kappa = 0.9700$. In the same figure a few of the low order periodic orbits are signaled by colored O and X marks for linear elliptic and hyperbolic stability, respectively. It can be observed that the line $x = 0$ contains only linear elliptic periodic points and for this reason is called the *dominant* symmetry line[4], although sometimes the name is also used also for the $x = 1/2$ line.

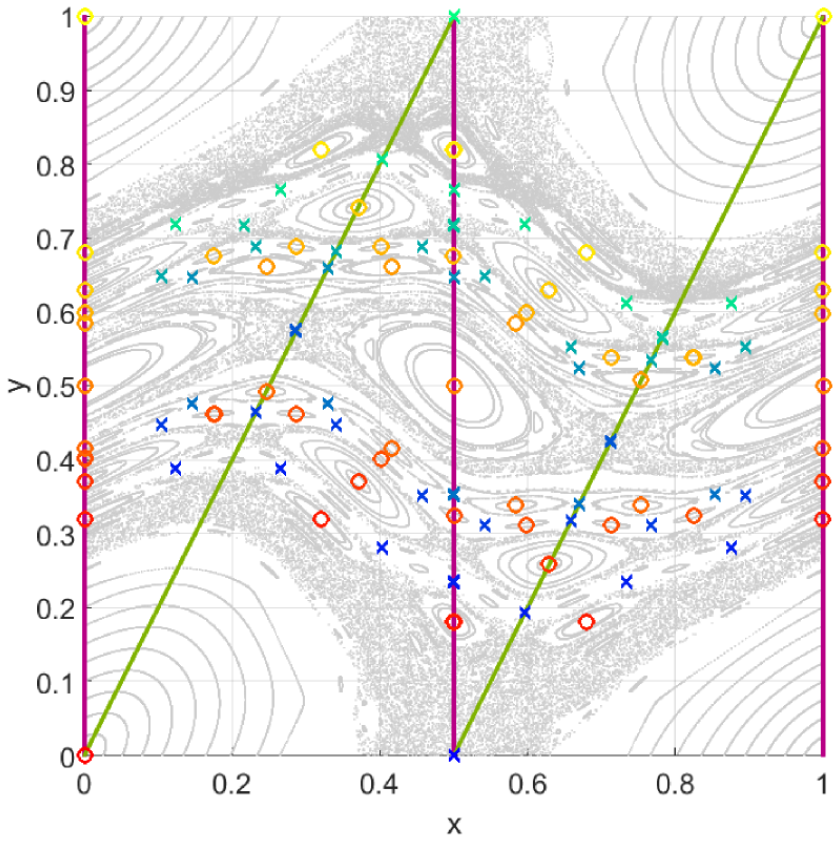

Figure 1: Example of symmetry lines and periodic orbits in the Chirikov-Taylor map (4) with $\kappa = 0.97$. The purple lines correspond to the symmetry lines of I_1 and green lines to symmetry lines of I_2. The search is one dimensional since all the monotone periodic orbits have at least one point in one of the symmetry lines.

The computation of high order periodic orbits allowed Greene to conjecture that the persistence of a given invariant circle R_ω is related to the stability of the periodic orbits of

rotation numbers p_n/q_n, when $p_n/q_n \to \omega$ as $n \to \infty$. Greene introduced a *residue*,

$$R = \frac{1}{2}[2 - \mathrm{Tr}(DT^q)]\,. \tag{6}$$

to characterize the linear stability of a periodic orbit of period q.

The work done by Greene on twist (reversible) maps was extended to non-twist maps [12, 14, 11] and other more general cases [32] but always in problems with symmetries for which it is possible to reduce the search of periodic orbits to one dimension.

Studies of the same kind for maps in higher dimensions (like Refs. [16, 17]) or two dimensional maps without symmetry lines have to search the periodic orbits in at least two dimensions, where the basins of attraction more often than not have a very complicate (fractal) structure[34] which makes methods like a 2D-Newton very unstable and sometimes unreliable unless the seed is already very close to the periodic orbit. On the other hand, the problem of the computation of periodic orbits using continuation methods can be very complex[34, 17] due the adjacent invariant structures like invariant manifolds. This problem has been sometimes approached by reducing the search to orbits with some kind of symmetry, as in Ref. [22] with the sequential periodic orbits (SPO's), but the results rarely are as general as in the work of Greene.

A *non-reversible map* should be any map that is not possible to rewrite as the composition of two involution, however in the present work it refers to any map for which there is no known decomposition (into two involutions). It is an open problem to characterize when it is possible to write a map as a composition of two involutions. Moreover the invariant sets of the involutions must be rather simple to use them as a guide to compute for the search of periodic orbits, Ref. [35] contains several cumbersome examples of symmetry lines of reversible maps.

In addition to the standard map we will use a standard-like map with perturbation function,

$$V'(x) = \frac{\kappa}{2\pi}\left(f(x) - \int_0^1 f(s)ds\right)\,, \qquad \text{where} \quad f(x) = \frac{\sin(2\pi x + p_a)}{1 - p_m\cos(2\pi x)}\,. \tag{7}$$

to illustrate the method. We refer to this map as the *rational harmonic* map due the form of the perturbation function. Note also that for $p_m \neq 0$ the perturbation function $V'(x)$ can be expressed as an infinite series of Fourier harmonics and is singular at $p_m = 1$. This map was studied before by [36] and [32] to test different kind twist maps universality results. Recently it was possible to find a generic two involutions decomposition of this map following Ref. [37], however the invariant sets of this generic involutions are not useful to compute periodic orbits, so for all the intended purposes this map is treated as non-reversible. Only for $p_a = 0, \pi$ it is possible to find symmetry lines similar to the standard map. The numerical continuation

for this map in Ref. [32] was found to be very sensitive to the variation of parameters p_a and p_m.

This map can help to study the role of reversibility and persistence of symmetry lines in twist maps and we believe it has not been studied in detail in the past due its apparent lack of symmetries.

3 The parameterization method

The paramererization method was originally introduced by de la Llave et al.[20] to find an approximate conjugation function between an invariant torus and the rigid rotation over a ideal torus. The rationale of the method is best understood in the constructive proof of the KAM theorem in Ref. [20], which relies among other things on a Newton iteration in the spirit of Nash-Moser theory, see Ref. [38]. A second ingredient for the particular implementation described here is related to the area preserving properties of the type of map considered that allows the use of a symplectic change of coordinates, referred in Ref. [20] as *automatic reducibility*.

Nash-Moser techniques can be used in algorithms that allow to continue smooth functions $K : \mathbb{S}^1 \to \mathbb{S}^1 \times \mathbb{R}$ satisfying the invariance equation,

$$T \circ K(\theta) = K(\theta + \omega)\,, \tag{8}$$

where $T : \mathbb{S}^1 \times \mathbb{R} \to \mathbb{S}^1 \times \mathbb{R}$ is a given twist map and ω is a Diophantine number, an irrational real number such that for a given τ there is a constant ν such that,

$$|\omega \cdot q - p| \geq \nu |q|^{-\tau},\ p \in \mathbb{Z},\ q \in \mathbb{Z} \setminus \{0\}\,. \tag{9}$$

Starting from the integrable case of the map T, the continuation moves the parameter as close to the breakdown of analyticity of the invariant circles as possible. The criterion of breakdown in Ref. [24] is used to determine when the invariant circle ceases to exist. This criterion states that close to the breakdown of analyticity the derivatives of the solution K start to blow up at points of $K(\mathbb{S}^1)$, in the sense that all the Sobolev $||\cdot||_{H^n}$ norms diverge.

Continuation methods like the one presented here have already been used in several contexts. See for instance, Ref. [18, 19], for models in statistical mechanics, Ref. [39, 40, 41] for examples in symplectic maps, Ref. [42, 43] for conformally symplectic models, and Ref. [44] for volume preserving maps.

The main idea of the method is to start from an approximate solution of the invariance equation applied to T and then produce a "better" approximate solution by adding a small correction. K_0 is said to be approximately invariant if

$$e_0(\theta) = T \circ K_0(\theta) - K_0(\theta + \omega)\,, \tag{10}$$

where $\|e_0\|$ is a small function with respect to the norm $\|\cdot\|$ of the Banach space of smooth functions, that represent the error of the approximation.

An approximate solution is said to be "better" if it approximates the invariance equation (8) with a smaller error. The idea is to add a periodic function $\Delta : \mathbb{S}^1 \to \mathbb{R} \times \mathbb{S}^1$ so that $K_1(\theta) = K_0(\theta) + \Delta(\theta)$ has an error

$$e_1(\theta) = T \circ K_1(\theta) - K_1(\theta + \omega) \tag{11}$$

with $\|e_1\| \approx \|e_0\|^2$.

This is possible according to Nash-Moser theory, adding an appropriate correction Δ can provide an error satisfying the quadratic property above. The correction Δ that could be used, would solve the Newton step equation,

$$DT(K_0(\theta))\Delta(\theta) - \Delta(\theta + \omega) = -e_0(\theta)\,, \tag{12}$$

which, if we were able to solve for Δ from equation (12), then the norm of the new error, $\|e_1\|$ will be of order $\|e_0\|^2$.

Taking into account the area preserving property of map T (the *automatic reducibility*), a change of coordinates $\Delta(\theta) = M_0(\theta)W(\theta)$, is applied to simplify (12). The new Newton step now requires to solve the equation,

$$\begin{pmatrix} 1 & S_0(\theta) \\ 0 & 1 \end{pmatrix} \begin{pmatrix} W_{(1)}(\theta) \\ W_{(2)}(\theta) \end{pmatrix} - \begin{pmatrix} W_{(1)}(\theta + \omega) \\ W_{(2)}(\theta + \omega) \end{pmatrix} = -M_0^{-1}(\theta + \omega)e_0(\theta). \tag{13}$$

where

$$M_0(\theta) = \left(\; DK_0(\theta) \;\middle|\; J^{-1}DK_0(\theta)N_0(\theta) \; \right)\,, \tag{14}$$

$$N_0(\theta) := [DK_0(\theta)^t DK_0(\theta)]^{-1}\,, \tag{15}$$

$$S_0(\theta) = N_0(\theta + \omega)DK_0^T(\theta + \omega)DF(K_0(\theta))DK_0(\theta)N_0(\theta)\,. \tag{16}$$

Its worth mentioning that the function $S_0(\theta)$ is related to the local twist condition on the invariant circle K_0.

Now, splitting the equation (13) into components there are two cohomological equations to be solved, namely[2]

$$W_{(2)}(\theta) - W_{(2)}(\theta + \omega) = -[M_0^{-1}(\theta + \omega)\mathbf{e}_0(\theta)]_{(2)} \tag{17}$$

[2]The subindices in parenthesis indicates the vector entry.

and

$$W_{(1)}(\theta) - W_{(1)}(\theta+\omega) = -[M_0^{-1}(\theta+\omega)e_0(\theta)]_{(1)} - S(\theta)W_{(2)}(\theta). \tag{18}$$

To solve the functional system of equations (17)-(18) in the Fourier space a necessary condition is that right hand side on both equations have average zero (or of the order of $O(\|e_0\|^2)$). This can be done easily for (18) since if the map is twist the average of W_2 is free parameter that can be adjusted as needed[3], however for the right hand side of (17) it is required that so by *Lemma 9* from Ref. [20],

$$\int_{\mathbb{S}^1} [M_0^{-1}(\theta+\omega)e_0(\theta)]_{(2)}\, d\theta = O(\|e_0\|^2)\,. \tag{19}$$

The reader is refered to the particular implementation of the method used in Ref. [23] for further details.

4 A new compound method

Note that the implementation of the parameterization method described in the previous section does not require the use of symmetry lines. However by construction the *standard* parameterization method can only approximate continuous objects. However in twist maps the monotone periodic orbits always exist for all values of the parameters (Birkhoff twist theorem and Aubry-Mather theory[1]), although these are discrete objects. Here we will use the parameterization method to approximate a curve that is not a dynamical object in all of its points, but that contains the periodic orbit and satisfies an invariance equation only at the points of the periodic orbit. By doing this, we are reducing the search of the periodic orbit to a lower dimensional object. This method is reminiscent of the search of periodic orbits using symmetry lines [3, 32].

When one naively attempts to apply the parameterization method to a non-Liouville rotation number the result will not converge due the "small denominators" problem and it is worse for rational rotation numbers, where there are "zero denominators". These zero denominators appear when we solve the following equation,

$$W(\theta) - W(\theta+\omega) = \tilde{e}(\theta+\sigma)\,, \tag{20}$$

where $\tilde{e}$ has zero average and σ is a phase to be determined. The zero denominators are due to the fact that we are looking for does not satisfy the invariance property in all of its points. In fact, the curve parameterized by K in this case, only satisfies the invariance condition (20) at the points that are on the periodic orbits. This fact leads to the functional equation

[3]If the map were not twist, it could be the case that $S_0(\theta) = 0$.

having no solution for all the points that do not correspond to the periodic orbit. At the same time there are infinitely many curves that satisfy the functional equation (20) at the points of the periodic orbit. In Fourier space, the solution of equation (20) is given by

$$a_k = \frac{b_k}{1 - e^{2\pi i \omega k}}, \qquad \text{if } e^{2\pi i \omega k} \neq 1\,. \tag{21}$$

with

$$W(\theta) = \sum_{k=-\infty}^{\infty} a_k e^{2\pi i k \theta}, \qquad \tilde{e}(\theta) = \sum_{k=-\infty}^{\infty} b_k e^{2\pi i k \theta}, \tag{22}$$

If $\omega = p/q$, then obviously $e^{2\pi i \omega k} = 1$ for $k = mq$ with $m \in \mathbb{Z}$. To solve the equations, we use the fact that the equations in Fourier space have solutions a_k as long as $k \neq mq$. Then we solve equation (20) in two steps. First, we look for the solutions (21) assuming that all $b_{mq} = 0$ for $m \in \mathbb{Z}$, and then we minimize the error only at the points corresponding to the periodic orbit by adjusting the phase σ. Thus, we use the parameterization method to find a continuous parametric curve $K(\theta)$ that contains all the periodic points (hyperbolic and elliptic) from the monotone periodic orbit $\omega = p/q$ up to an error of $O(||\tilde{e}||)$. In practice, we found that even though convergence of the method is not yet proven it provides a good approximation that can be used to find the periodic orbit with a Newton Gauss method that will be explained in Section 4.2.

A quantitative aspect not explicitly mentioned before is that the number of Fourier modes considered is for practical reasons always finite. However it is guaranteed by the theory behind the parametererization method that for a fixed upper bound for the error of the approximate solution, $||\tilde{e_1}|| < \tilde{\varepsilon}$ there is an optimal maximum number of Fourier coefficients $N(\tilde{\varepsilon})$ to be considered so the norm of the remaining tail of harmonics can always be safely included inside the error of the approximate solution[24]. A proof in the convergence of the new method is still pending so there is not a clear argument of how many harmonics is convenient to use. If the number of harmonics N^* is fixed a priori, then the method, when it converges, should give an optimal trigonometric polynomial of degree N^* such that the parametric curve pass close to the points of the periodic orbit. And even if the method does not converge and gives an approximate value of a point of the periodic orbit with a bounded error, it may suffice to be used as seed for 2-D methods. So a convergence theorem may not be needed at this point for the implementation of the method.

Although the hypothesis of existence of a parametric curve $K_{p/q}$ that cross all the points of the periodic orbits of rotation number p/q does not seem unreasonable for maps like the standard map (4) and probably any locally twist map, it is an open problem to prove its existence. The numerical evidence indicates that this is true and it should be possible to find a mathematical proof. Nevertheless the present work only focuses on the implementation of the hybrid method and on presenting numerical evidence.

If an existence theorem is proven or if its error can be bounded, an interesting question would be to relate properties such as the regularity of the parametric curves K_{p_n/q_n} to a K_ω, when $\{p_n/q_n\}_{n\in\mathbb{N}}$ is a sequence that converges to a Diophantine rotation number ω. A different approach could be to use an a posteriori theorem of the type of Refs. [45, 46, 47] to prove the existence and uniqueness of these periodic points.

4.1 Phase tracking

The method sketched is expected to yield a parametric curve $K_{p/q}$ that approximately contains the periodic orbit that we are looking for. The problem now is to find the correct phase $\tilde{\theta} \in [0, 1/2q_n)$ such that,

$$T^q(K_{p/q}(\tilde{\theta})) \approx K_{p/q}(\tilde{\theta})\,. \tag{23}$$

Applying Birkhoff's twist theorem[1] to the conjugation between the rigid rotation $\mathsf{R}_{p/q}$ ($\mathsf{R}_{p/q}(x) \equiv x + p/q$) and the map T via the parametererization function $K_{p/q}$,

$$T \circ K_{p/q} = K_{p/q} \circ \mathsf{R}_{p/q}\,, \tag{24}$$

there must exist at least $2q$ equidistant values of $\tilde{\theta}$ in $[0, 2\pi)$ that satisfy (23). There are cases in which there can be more than one set of elliptic (hyperbolic) fixed points connected by iteration of the map. However when the Aubry-Mather theory is applicable, it is guaranteed that there can only exist two monotone orbits for a fixed rotation number, one minimal orbit and one minimax orbit, see Ref. [1]. For the usual cases in the literature, it is only needed to find two independent $\tilde{\theta}_1$ and $\tilde{\theta}_2$ to be able to compute the complete the set of points with linear elliptic and hyperbolic stability that form the periodic orbits. Here, independent means that there is no $n \in \mathbb{Z}$ such that $\theta_2 = \theta_1 + np/q \mod 2\pi$, since if $K_{p/q}(\tilde{\theta}_1)$ is a periodic point then $K_{p/q}(\tilde{\theta}_1 + np/q)$, $n = 1, 2, ..., q$ have to be also periodic points of the same orbit, see Fig. 2.

There are two candidates to help find the *correct* phases $\tilde{\theta}$: the error of the approximate periodic point,

$$E(\theta) = ||T^q(K(\theta)) - K(\theta)|| \tag{25}$$

and Greene's residue $R(\theta)$,

$$R(\theta) = \frac{1}{4}\Big[2 - \mathrm{Tr}\Big(DT^n(K(\theta))\Big)\Big]\,. \tag{26}$$

for $\theta \in [0, 2\pi]$, however it is enough to restrict the search for $\theta \in [0, p/q]$. The minima of $E(\theta)$ should indicate the points in the curve $K(\theta)$ that are closer to the actual periodic points and $R(\theta)$ which change of signs should indicate the regions in which it should be possible to find approximate solutions of different linear stability.

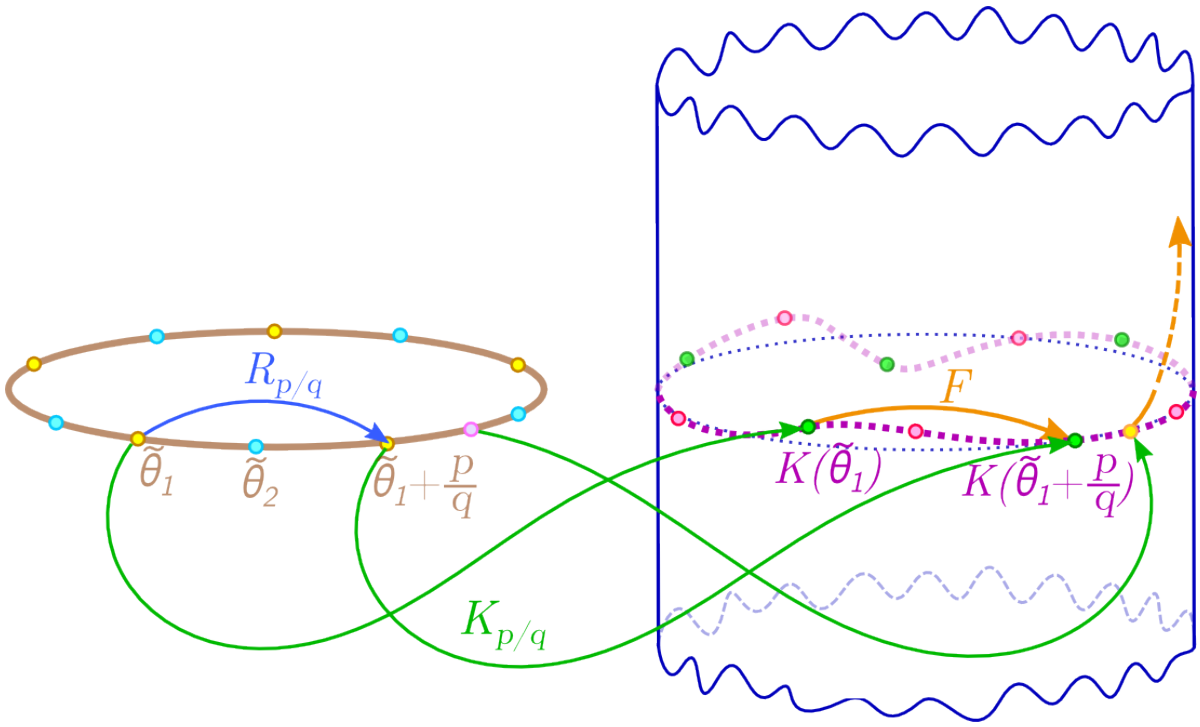

Figure 2: Illustration of the components of the modified parameterization method, for which the parameterization $K_{p/q}$ is only dynamically consistent with the map T for periodic orbits points.

Both quantities, $E(\theta)$ and $R(\theta)$, present problems in their computation and $R(\theta)$ in particular has a very well known unstable behavior when computed *not close enough* of a periodic orbit. Nevertheless the underlying idea behind the parameterization method is that the exact dynamic of the map T is conjugated to a rigid rotation over a parametric curve K. So it is reasonable to expect for our case is that for $\theta \in (\theta_i - \delta, \theta_i + \delta)$, where θ_i are independent solution of (23), the dynamic of $T(K(\theta))$ will be also approximated by the conjugation,

$$T(K_{p/q}(\theta)) \approx K_{p/q}(\theta + p/q)\,, \tag{27}$$

while for other values of θ the dynamic may radically differ. The later points of the parametric curve are not relevant for the search of periodic orbits and can be disregarded for now. The benefit of using the dynamic of the conjugation (24) is to compute approximate versions $E(\theta)$ and $R(\theta)$ is that both will be computed over smooth functions over bounded (compact) domains, so both are expected to be also regular. Then we define,

$$\tilde{E}(\phi) = ||K_{p/q}(\theta + p) - K_{p/q}(\theta)|| \tag{28}$$

$$\tilde{R}(\theta) = \frac{1}{2}[2 - \mathrm{Tr}(\tilde{\mathcal{M}}^q(\theta))]\,, \tag{29}$$

where $\tilde{\mathcal{M}}^q(\phi)$ is the *regularized* Jacobian matrix of T^q, computed as,

$$\tilde{\mathcal{M}}^q(\phi) = DT[K_{p/q}(\theta + (q-1)p/q)] \cdots DT[K_{p/q}(\theta)]\,. \tag{30}$$

The computation of the residue by the iteration of the map and its linear approximation (Jacobian matrix) can diverge for small errors in the initial data of a periodic orbits, giving values of order 10^{50} for orbits of periods of order of 10^2. In contrast, the approximate computation via the conjugation function K will keep the estimation always bounded. Letting, for example, compute a small residue of order 10^{-15} even if the error on the orbit is of order 10^{-5} (for a period of order 10^2).

$\tilde{E}(\theta)$ and $\tilde{R}(\theta)$ are expected to be more regular than their exact counterparts $E(\theta)$ and $R(\theta)$ for the above mentioned reasons, however the numerical implementation of (28) was found not optimal for high order periods ($q \gtrsim 10^3$), yielding small values close to the machine precision[4]. So instead, the following two error estimators are used,

$$\hat{E}_1(\theta) = \sum_{n=0}^{q-1} |T \circ K(\theta + np/q) - K[\theta + (n+1)p/q]|\,, \tag{31}$$

$$\hat{E}_2(\theta) = \left\{ \sum_{n=0}^{q-1} \{T \circ K(\theta + np/q) - K[\theta + (n+1)p/q]\}^2 \right\}^{1/2}. \tag{32}$$

These error functions are also regular for the same reason as $\tilde{E}$ but yield not too small values thanks to the sum over all the iterates, see the blue curve in Fig. 3. Although in the numeric calculations of high order periods ($q \gtrsim 10^3$), $\hat{E}_1$ is better behaved for values close to machine precision.

The regularity of the function $\tilde{R}$ and the fact that it should be positive (negative) close to the elliptic (hyperbolic) periodic points, guarantees that $\tilde{R}$ is an oscillatory function with mean close to zero, as it can be appreciated in the red curve in Fig. 3.

As it can be appreciated in Fig. 3, it was found for all the computed cases that the minima $\{\theta_n^{(min)}\}_{n=1,\ldots,2q}$ of $\hat{E}_1$ are placed always in the vicinity of the maxima and minima $\{\theta_n^{(crit)}\}_{n=1,\ldots,2q}$ of $\tilde{R}$. The numerical evidence consistently suggest that there exist an analytic relation between the critical points of $\tilde{R}$ and the minima of $\hat{E}_1$ but there is not yet a complete proof to this fact. The numerical evidence is in agreement with preliminary results of an a posteriori Newton-Kantorovich theorem of the type Refs. [47] that relates the critical points of the approximate residue $\tilde{R}$ with the existence of periodic orbits. The a posteriori theorem

[4]We are working with quadruple precision.

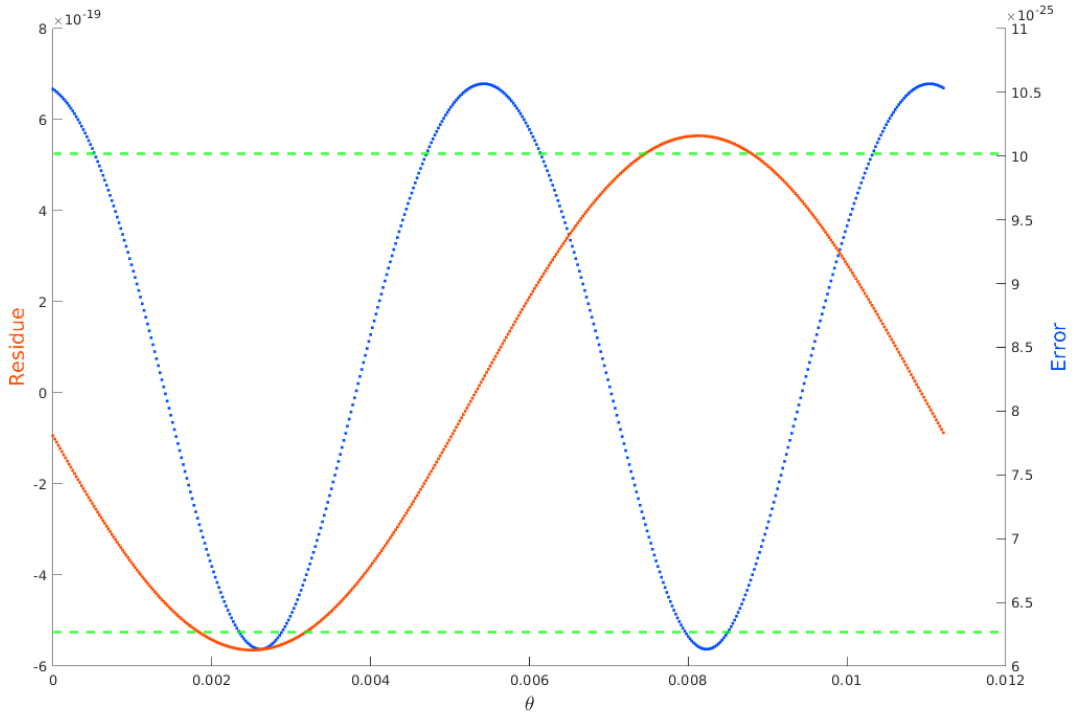

Figure 3: Error $\hat{E}_1$ (blue) and regularized residue $\tilde{R}$ (red)of the approximated solution for the 55/89-periodic orbit of the *rational harmonic map* (7) with the values of the parameters: $\kappa = 0.4$, $p_a = 2.5$ and $p_m = 0.37$. The green dashed horizontal lines correspond to the exact value residue for the hyperbolic (-5.253×10^{-19}) and elliptic (5.254×10^{-19}) orbits.

guarantees the existence of a unique fixed point (a periodic orbit point for $G(x) = T^q(x) - x = 0$) in an open ball $B_r(\bar{x})$ around of a given $\bar{x}$, if some bounds hold and a polynomial function of these bounds on r admits negative values for $r > 0$. Restricting the theorem to the present case, the polynomial function have the form,

$$\mathfrak{p}(r) = Z_2(r)r^2 - r + Y_0\,, \tag{33}$$

where $Z_2(r)$ is a positive function of r and Y_0 is positive real constant that in their definition appear the modulus of the residue R dividing. So it is more likely for $\mathfrak{p}(r)$ to be negative in an interval $(0, \tilde{r})$ for $\bar{x} = K_{p/q}(\theta)$ around the critical points of $\tilde{R}(\theta)$ for which Z_2 and Y_0 are smaller. This not a proof but an argument that will be addressed in a future work.

Although there is not yet a complete explanation of this "numerical coincidence", it is convenient to use the critical points of $\tilde{R}$ as an estimator of the position $\tilde{\theta}_n$ of the periodic

points in $K_{p/q}(\theta)$ when $\hat{E}_1$ is unreliable due to numerical error.

Table 1 displays data from a few periodic orbits of the Chirikov-Taylor map, in which it is possible to observe the agreement between the minima of $\hat{E}_1$ and the critical points of $\tilde{R}$.

$\frac{p}{q}$		$\hat{E}_{1,min}$	x_{min}	$\tilde{R}_c$	x_c	$\lvert x_{min} - x_c \rvert$
$\frac{5}{8}$	(h)	1.689×10^{-10}	0.000×10^{-00}	2.520×10^{-01}	0.000×10^{-00}	0.00×10^{-00}
	(e)	1.689×10^{-10}	6.250×10^{-02}	-2.573×10^{-01}	6.250×10^{-02}	0.00×10^{-00}
$\frac{55}{89}$	(h)	3.118×10^{-08}	0.000×10^{-00}	2.133×10^{-01}	0.000×10^{-00}	0.00×10^{-00}
	(e)	3.079×10^{-08}	5.595×10^{-03}	-2.172×10^{-01}	5.618×10^{-03}	2.30×10^{-05}
$\frac{377}{610}$	(h)	6.762×10^{-10}	0.000×10^{-00}	8.328×10^{-02}	0.000×10^{-00}	0.00×10^{-00}
	(e)	6.404×10^{-10}	8.098×10^{-04}	-8.391×10^{-02}	8.197×10^{-04}	9.90×10^{-06}
$\frac{987}{1597}$	(h)	2.015×10^{-11}	0.000×10^{-00}	1.380×10^{-02}	0.000×10^{-00}	0.00×10^{-00}
	(e)	1.909×10^{-11}	3.093×10^{-04}	-1.381×10^{-02}	3.131×10^{-04}	3.80×10^{-06}

Table 1: Comparison of the localization in the angular variable $x(\theta)$ of two adjacent local minima of $\hat{E}_1(\theta)$, the ℓ^2-norm of the error function (32), and two adjacent critical points of $\tilde{R}(\theta)$, the regularized residue defined in Eq. (29) for a few periodic orbits of the Chirikov-Taylor map (4) with $\kappa = 0.9700$, computed by the *modified parameterization method*. (h) and (e) correspond respectively to a linear hyperbolic and elliptic points.

4.2 Newton method

In this section we describe a Newton-like method to calculate (or refine) periodic orbits of high order with high precision. The method here described was developed by À. Haro and collaborators [48].

Now lets assume we have an approximation $\tilde{\mathcal{Z}}$ of the periodic orbit $\mathcal{Z}$. Then, on the lift, the points $\tilde{z}_i \in \tilde{\mathcal{Z}}$ satisfy the equations,

$$\begin{cases} T(\tilde{z}_{q-1}) - \tilde{z}_0 &= \mathsf{e}_0 + P\,, \\ T(\tilde{z}_0) - \tilde{z}_1 &= \mathsf{e}_1\,, \\ &\vdots \\ T(\tilde{z}_{q-2}) - \tilde{z}_{q-1} &= \mathsf{e}_{q-1}\,. \end{cases} \tag{34}$$

where $\mathsf{e}_i \in \mathbb{R}^2$, $||\mathsf{e}_i|| \ll 1$ for $i = 0, 1, \ldots, q-1$ and P is the same from (1).

To find the periodic orbit $\mathcal{Z}$ we need to find the roots of (34), i.e. $\{\tilde{z}_0, \tilde{z}_1, \ldots, \tilde{z}_{q-1}\}$ such that the errors e_k are zero. Labeling the right hand side of (34) as a function $G(\tilde{z}_0, \ldots, \tilde{z}_{q-1}) : \mathbb{R}^{2q} \to \mathbb{R}^{2q}$, the problem to solve is $G(\tilde{z}_0, \ldots, \tilde{z}_{q-1}) = 0$. Using the notation of $\mathbf{z} =$

$(z_0, \ldots, z_{q-1})^t$ to refer a $2q$ vector which components correspond to the concatenation of the components of the points of a given $\mathcal{Z}$, the standard Newton method to solve the problem consist in the contracting map,

$$\hat{\mathbf{z}} = \tilde{\mathbf{z}} - DG^{-1}(\tilde{\mathbf{z}}) \cdot G(\tilde{\mathbf{z}}) \,, \tag{35}$$

where $\tilde{\mathbf{z}}$ is assumed to be inside an open ball sufficient small of a root $\mathbf{z}_*$ of $G(\mathbf{z}_*) = 0$.

Labeling $\Delta = \hat{\mathbf{z}} - \tilde{\mathbf{z}}$ and using (34) to identify $G(\tilde{\mathbf{z}}) = \mathbf{e} = (\mathsf{e}_1, \ldots, \mathsf{e}_{q-1})^t$, Eq. (35) can be written as,

$$DG(\tilde{\mathbf{z}})\Delta = -\mathbf{e} \,, \tag{36}$$

where $DG(\tilde{\mathbf{z}})$ is a $2q \times 2q$ matrix. In more detail (36) has the form,

$$\begin{pmatrix} -I & \bigcirc & \bigcirc & \ldots & \bigcirc & DT(z_{q-1}) \\ DT(z_0) & -I & \bigcirc & \ldots & \bigcirc & \bigcirc \\ \bigcirc & DT(z_1) & -I & \ldots & \bigcirc & \bigcirc \\ \vdots & \vdots & \ldots & \ddots & \vdots & \vdots \\ \bigcirc & \bigcirc & \bigcirc & \ldots & DT(z_{q-1}) & -I \end{pmatrix} \begin{pmatrix} \Delta z_0 \\ \Delta z_1 \\ \Delta z_2 \\ \vdots \\ \Delta z_{q-1} \end{pmatrix} = \begin{pmatrix} -\mathsf{e}_0 \\ -\mathsf{e}_1 \\ -\mathsf{e}_2 \\ \vdots \\ -\mathsf{e}_{q-1} \end{pmatrix} , \tag{37}$$

where I is the 2×2 identity matrix, $\bigcirc$ the 2×2 zero matrix and $DT(z_j)$ for the Jacobean matrix of the map T evaluated at z_j. It is important to note that $DG(\tilde{\mathbf{z}})$ is sparse because it only contains the diagonal plus 3 subsequent inferior and the last 2 right columns.

To solve the system (37), we choose the Gauss method on the columns, since for each step of the Gauss method the structure of matrix $DG(\tilde{\mathbf{z}})$ is preserved. The original and final matrix can be visualized schematically as in Fig. 4.

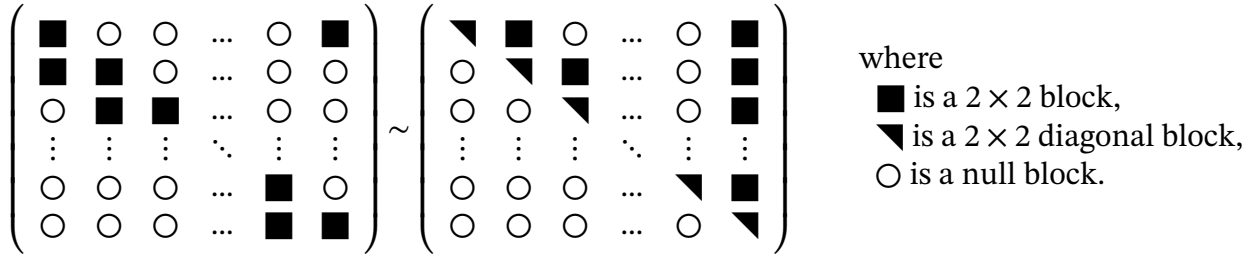

Figure 4: Scheme of the matrix from Eq. (37) before and after triangularization.

It must be noted that the memory storage of this procedure is proportional to q (for an orbit of period q we need $12q + 4$ memory locations to storage the $DG(\tilde{\mathbf{z}})$ matrix) and $4q$ locations to storage the vectors Δ and $\mathbf{e}$.

The usual implementation of the Newton method to find a periodic orbit of rotation number p/q consists in finding the root of a function $\mathcal{G}(z) = 0$ taken from (1),

$$\mathcal{G}(z) = T^q(z) - z - P = 0\,, \tag{38}$$

where $z \in \mathbb{R}^2$. The Newton's method iteration for this problem is,

$$z_{i+1} = z_i - ((DT^q)^{-1}(z_i))\mathcal{G}(z_i) \tag{39}$$

where, by the chain rule, $DT^q(z) = DT(T^{q-1}(z)) \cdot DT(T^{q-2}(z)) \cdots DT(T(z)) \cdot DT(z)$. This implementation of the standard Newton's method seems simpler since the dimension of z is just two. However the standard Newton method is known to be highly unstable for maps of 2 or higher dimensions and it is almost unreliable to find periodic orbits of period higher than 10^3.

The first implementation described in this section, that we call *Newton-Gauss* method, allows to find periodic orbits of period $\lesssim 10^7$ with the use of quadruple arithmetic precision. The *Newton-Gauss* method shows to be very stable and allows to perform procedures of continuation of the orbits by varying the parameters. The robustness of the method relies on the fact that we solve (by Gauss method) **one** iteration of the Newton method for **one** iteration of the map on every point of the orbit at the same time, much like in the way of the collocation methods. Also it must be mention that the Newton-Gauss method is extraordinary fast and computationally cheap in terms of the required memory storage. This method can also be used as a continuation method by doing small variation of the parameters.

4.3 The compound method

Summarizing the method described in this section and taking into account the numerical evidence given by earlier implementations, the parameterization method is modified into the following algorithm described below.

Algorithm 1.

1) Let $e_0(\theta) = T \circ K_0(\theta) - K_0(\theta + P/Q)$.

2) Compute the matrix $M(\tilde{\theta})$ *from equation* (14).

3) Solve for $W_2(\tilde{\theta})$ *from* (17)*, after eliminating all resonant terms of the Fourier series of* e_0 *and* W_2*, that is the terms of the form* $c_{nQ}e^{\pm inQ\tilde{\theta}}$.

4) Choose the average $\int_{\mathbb{S}^1} W_2(\theta)d\theta$ *so that* $-[M_0^{-1}(\theta+\omega)e_0(\theta)]_1 - S_0(\theta)W_2(\theta)$ *has an average close to zero.*

5) *Solve for* $W_1(\tilde{\theta}_0)$ *from* (18)*, eliminating all the resonant terms.*

6) *Compute the step* Δ*,*

$$\Delta(\tilde{\theta}) = M_0(\tilde{\theta})W(\tilde{\theta})$$

7) *Obtain the new parameterization* K_1*,*

$$K_1(\theta) = K_0(\theta) + \Delta(\theta)$$

8) *Set* $K_0(\theta) = K_1(\theta)$ *and go to step 1) until an a priori fixed bound* $|\min e_0(\theta)| < T$ *is satisfied.*

9) *Find two adjacent local minimum and maximum* $\left\{\tilde{\theta}_1, \tilde{\theta}_2\right\}$ *of* $\tilde{R}(\theta)$[5]*.*

10) *Apply the Newton-Gauss method (35)-(37) to* $(x_0, y_0) = K_0(\tilde{\theta}_k)$*,* $k = 1, 2$ *to obtain a point from each one of the hyperbolic and elliptic periodic orbits with the required precision.*

The steps $1) - 10)$ from algorithm 1 will be called the *modified parameterization method* and the 11) the Newton-Gauss method.

5 Implementation of the compound method

To test the capabilities of the compound method as a continuation method to obtain periodic orbits, first we tested the *modified parameterization method* (MPM) alone on the Chirikov-Taylor map. The continuation started from the integrable case ($\kappa = 0$) to the neighborhood of the critical κ^*. From earlier tests of the code it was found the need to perform the computations with quadruple precision ($O \sim 10^{-30}$), particularly in the FFT computation. Figure 5 shows the error $\tilde{E}_1$ as function of the perturbation parameter κ. Notice that the order of the initial flat part of the graphs in the figure are around machine error ($O \sim 10^{-30}$) and should be considered spurious.

A first observation from Fig. 5 is that the error of E grows as a power of κ to a given exponent. This is to be expected since the *modified parameterization method* is attempting to approximate with a smooth continuous curve a periodic orbit that tends to have a self-similar (fractal) structure as $\kappa \to \kappa_G$ and the period q increase. The next feature appreciable in Fig. 5 and 6, that seems counter intuitive, is that for $\kappa < \kappa_G$ the error reduces as the period of the orbit increase. Although this is easily explained by considering that the stability of the

[5]We chose to find extrema of the residue as opposed to finding minima of the error since we obtained better results in this manner.

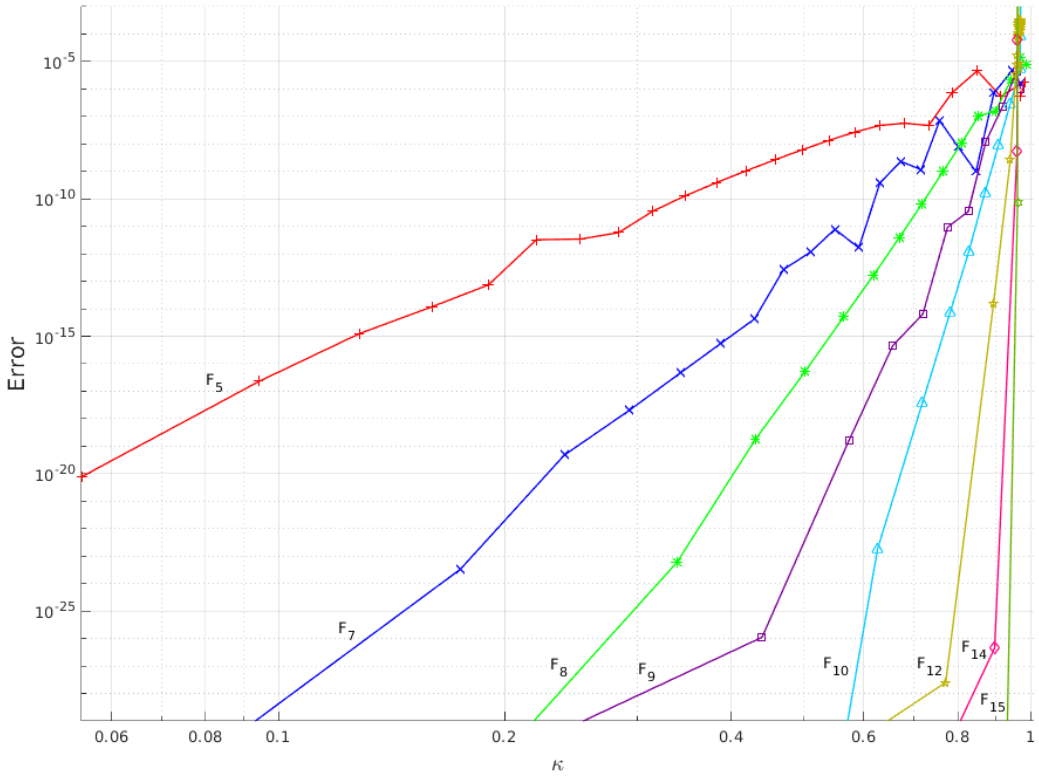

Figure 5: Global minimum of the error $\hat{E}_1$ of the approximated solution for the Chirikov-Taylor map (4) as function of the parameter κ using only the *modified parameterization method* for different rotation numbers corresponding to Fibonacci ratios F_{N-1}/F_N from $N = 5$ to $N = 15$.

periodic orbit, given by the residue, modulates the behavior of the error (Fig. 7). It can also be appreciated from Fig. 5 that working in quadruple precision, the *modified parameterization method* gives reasonable good estimates of the periodic orbits for values of κ away from the critical. The 2D-Newton method may only be required, depending of the precision needs, for calculations where the modulus of the residue of the periodic orbit is greater than 10^{-12}.

As a complement to the error behavior, the amplitude of the approximate residue $\tilde{R}$ of the computed periodic orbits behaves as expected. Fig. 7 displays the amplitude of the approximate residue $\tilde{R}$ of the same periodic orbits from Fig. 5 but with the refining of the Newton-Gauss method. Even for the unrefined periodic orbit data, the four lowest

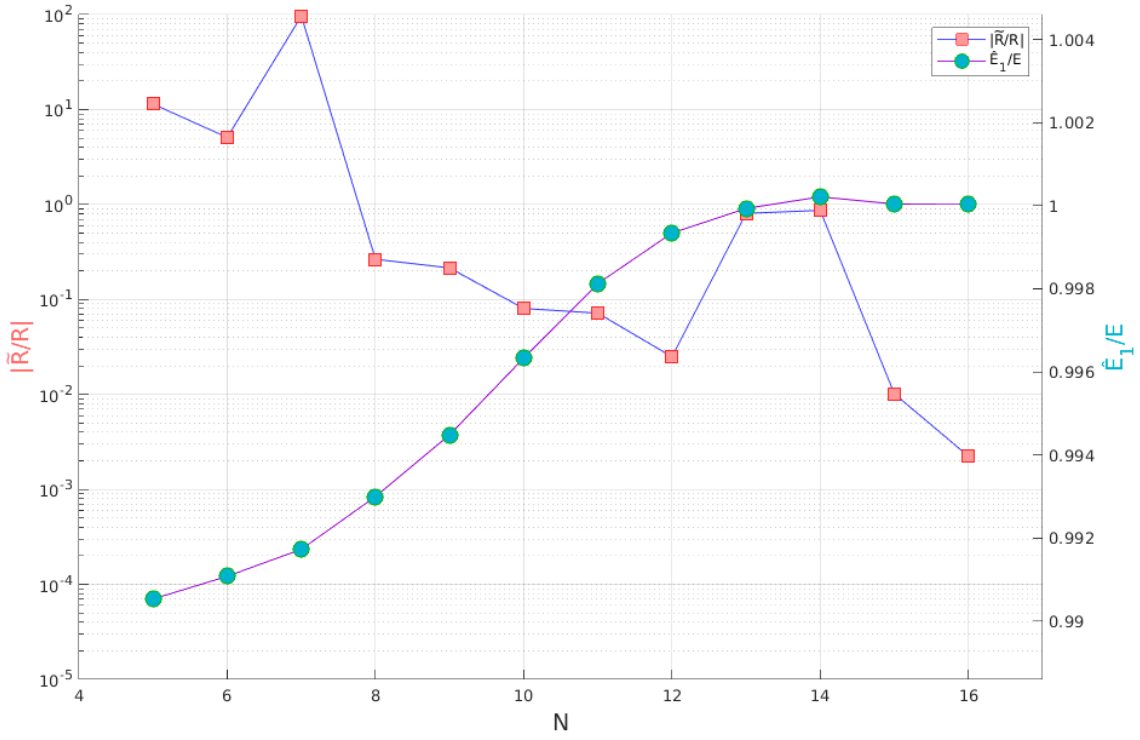

Figure 6: Ratio of errors $\hat{E}_1/E$ and residues $|\tilde{R}/R|$ for the first F_{N-1}/F_N hyperbolic periodic orbits that approximate the golden mean invariant circle in the Chirikov-Taylor map (4) for $\kappa = 0.9600$, computed by the modified parameterization method alone. N correspond to the rotation number of the orbit F_{N-1}/F_N.

order periodic orbits that incidentally have the lowest error near the critical region, cross at $\kappa \approx 0.971$ and $\max |\tilde{R}| \approx 0.25$.

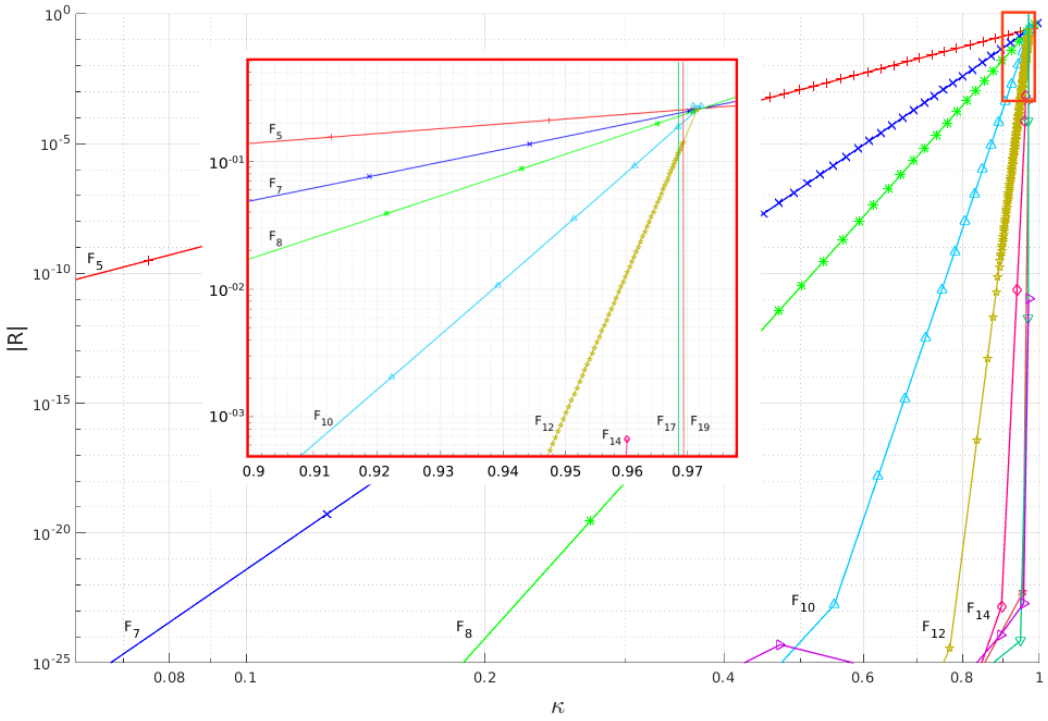

Figure 7: Amplitude of $\tilde{R}$ of the approximated solution for the standard map (4) as function of the parameter κ, for different rotation numbers corresponding to Fibonacci ratios F_{N-1}/F_N from $N = 5$ to $N = 20$ using the compound method.

6 Results

The compound method was tested for two symplectic maps: the standard map (4) (in the Chirikov-Taylor map case) and a three parameter rational harmonic map (7) with no useful decomposition into two involutions for a generic values of the parameters. The results are presented in this section.

6.1 Standard map

The first test of the *compound method* was done over the Chirikov-Taylor map Eq. (4) to compare with the orbits obtained via symmetry lines algorithms. The purpose of the test is to identify some problems of the code implementation of the compound method and give

bounds to the free parameters of the method like the number of Fourier modes, continuation step size and others, and the same time compare the execution run times and check if the desired precision can be attained. Additionally the test discovered the surprising agreement between the critical points of $\tilde{R}$ and the minima of $\hat{E}$. Also it was possible to compare the difference between using different number N^* of harmonics in the approximation. For small values of Q, the total number of harmonics N^* was taken as $2Q$, while for larger values $N^* \sim 4Q$. Increasing the value of N^* over $4Q$ did not reflect in a better convergence of the method and in some cases increase it since the extra terms were spurious.

The results of performing a first numerical continuation by the *modified parameterization method* and then using the data as seed for the 2D-Newton method are contained in table 2.

With the use of the Newton-Gauss method, it was possible to find periodic orbits of higher periods close the critical parameter value.

6.2 Rational harmonic map (RHM)

The map has the symmetry

$$(x, y; \kappa, p_a, p_m) \mapsto (x - 1/2, y; \kappa, p_a + \pi, -p_m)\,, \tag{40}$$

which can be used to reduce the search in the parameter space from $\mathbb{R}^3$ to $\mathbb{R}^2 \times \mathbb{R}^+$.

Before exploring the the whole parameter space it is convenient to verify that the critical behavior of the rational harmonic map agrees with what is observed for the standard map, in particular Greene's residue behavior of continuous lines in Fig. 8, for the same rotation numbers that approximate the golden mean F_{n-1}/F_n. The dashed lines in Figure 8 shows the behavior of the residue R for different rotation numbers computed for a continuation on parameter κ from the integrable case $\kappa = 0.0$ for $((p_a, p_m) = (3.0, 0.4))$. It can be appreciated in the figure that the residue of the different rational rotation numbers[6] cross around $R \sim 0.25$ for $\kappa = 1.72$ with apparent same power laws as in the standard map. This can be appreciated in Fig. 8 in which the perturbation parameter κ from the RHM has been re-scaled to match the standard map. Notice that the apparent critical value of the residue remains the same in both cases and also with the same slope for each rotation number.

With the purpose to corroborate that RHM fulfills the renomalization theory from Greene and MacKay, we performed a numerical experiment. The renormalization theory assure us that for critical values of the parameters, i.e. the the values of breaking of the invariant circle ω, every periodic orbit with rotation number p_n/q_n such that $p_n/q_n \to \omega$ have the **same** value of the residue (6). Therefore we searched the parameter space of the RHM on regular grid of values of (p_a, p_m) for the critical value or $\kappa*$ such that different periodic orbits with

[6]Fibonnacci sequence ratios $\{F_{m-1}/F_m\}$ that approximate the golden mean.

$\frac{p}{q}$	Orbit x	E	R
$\frac{5}{8}$	$1.04262381263415710544 \times 10^{-01}$	1.7776×10^{-33}	-2.3618×10^{-01}
$\frac{8}{13}$	$7.2292421040641022513 \times 10^{-02}$	3.8240×10^{-45}	-2.1396×10^{-01}
$\frac{13}{21}$	$5.06992260762055879603 \times 10^{-02}$	1.4227×10^{-30}	-1.9779×10^{-01}
$\frac{21}{34}$	$3.5022447826195364453 \times 10^{-02}$	3.0469×10^{-30}	-1.6521×10^{-01}
$\frac{34}{55}$	$2.4048789198498598295 \times 10^{-02}$	1.5432×10^{-29}	-1.2748×10^{-01}
$\frac{55}{89}$	$1.62171825022147208409 \times 10^{-02}$	2.8721×10^{-32}	-8.2110×10^{-02}
$\frac{89}{144}$	$1.0731773004662365072 \times 10^{-02}$	6.7440×10^{-52}	-4.0823×10^{-02}
$\frac{144}{233}$	$6.9344882456917456713 \times 10^{-03}$	5.2130×10^{-55}	-1.3101×10^{-02}
$\frac{233}{377}$	$4.39068507873134101191 \times 10^{-03}$	1.9267×10^{-32}	-2.0969×10^{-03}
$\frac{377}{610}$	$2.74217144026659842688 \times 10^{-03}$	9.5578×10^{-30}	-1.0800×10^{-04}
$\frac{610}{987}$	$1.70222914399736324091 \times 10^{-03}$	9.8163×10^{-45}	-8.9147×10^{-07}
$\frac{987}{1597}$	$1.05402094177906953965 \times 10^{-03}$	6.5275×10^{-46}	-3.7914×10^{-10}

Table 2: Angular component x of the closest point to $x = 0$ of the first few golden mean approximates P/Q hyperbolic periodic orbits of the Chirikov-Taylor map (4) for $\kappa = 0.9600$, computed by the modified parameterization method (table 6) and then refined by a 2D-Newton method up to $|E| < 10^{-28}$.

rotation numbers F_{n-1}/F_n would have the same residue $|R| \sim 0.2554$. If the renormalization is right, for the same values of (p_a, p_m) different periodic orbits must have the same critical $\kappa*$ and the same critical residue value reported for the golden mean in the standard map.

The compound method (modified parameterization method (MPM) and then the Newton-Gauss method) was used continuation method over the parameter κ starting from the integrable case $\kappa = 0$ over an uniform mesh in (p_a, p_m) for different rotation numbers corresponding to Fibonnacci ratios F_{n-1}/F_n. The stopping criteria for the continuation is that the residue of the orbit outgrows the critical threshold predicted by Greene and MacKay ($|R| \sim 0.2554$) or that the error E_1 can not be reduced by the Newton step of the parameter-

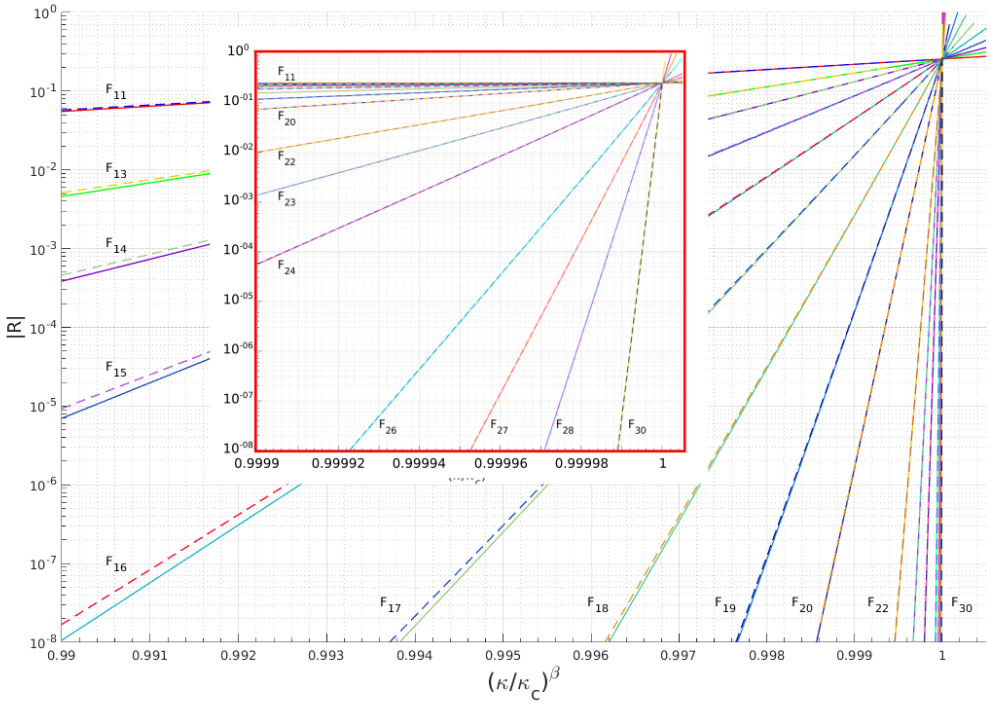

Figure 8: Comparison between the residues R of periodic orbits for the standard map (continuous lines) and the rational harmonic map (dashed lines) (7) for $(p_a, p_m) = (3.0, 0.4)$, both as function of a scaled parameter $(\kappa/\kappa_c)^\beta$. Where $(\kappa_c, \beta) = (0.9716354, 1.0)$ for the standard map and $(\kappa_c, \beta) = (1.73360453, 1/1.13)$ for the RHM. The orbits rotation numbers correspond to the Fibonacci ratios F_{N-1}/F_N from N=11 (89/144) to N=30 (832040/1346269).

ization method bellow an a priori fixed upper bound $E_1 \lesssim 10^{-18}$. The use of the symmetry (40) helped to reduce the search in the parameter space. The critical manifold found for F_{15}/F_{16}, the 987/1597-periodic orbit, can be appreciated in Figs. 9, and 10.

It can be appreciated from Fig. 9 that the behavior of the critical value of κ as function of p_m seems to agree with the expected from the perturbation function (7), bigger values of p_m should yield lower values of κ_*. It is however unexpected to find that for $p_a \sim \pi$ there appear irregularities that suggest that the critical surface may have folds and also, in the same region, κ_* rise to values bigger than the critical $\kappa_* = \kappa_G$, the analytic critical value for $p_m = 0$ and any p_a. Because of this peculiar behavior of the manifold, it was chosen to compute periodic orbits for $(p_a, p_m) = (3.0, 0.4)$, close to a fold but yet not the reversible case of $p_a = \pi$. Some of the computed orbits are presented in table 3.

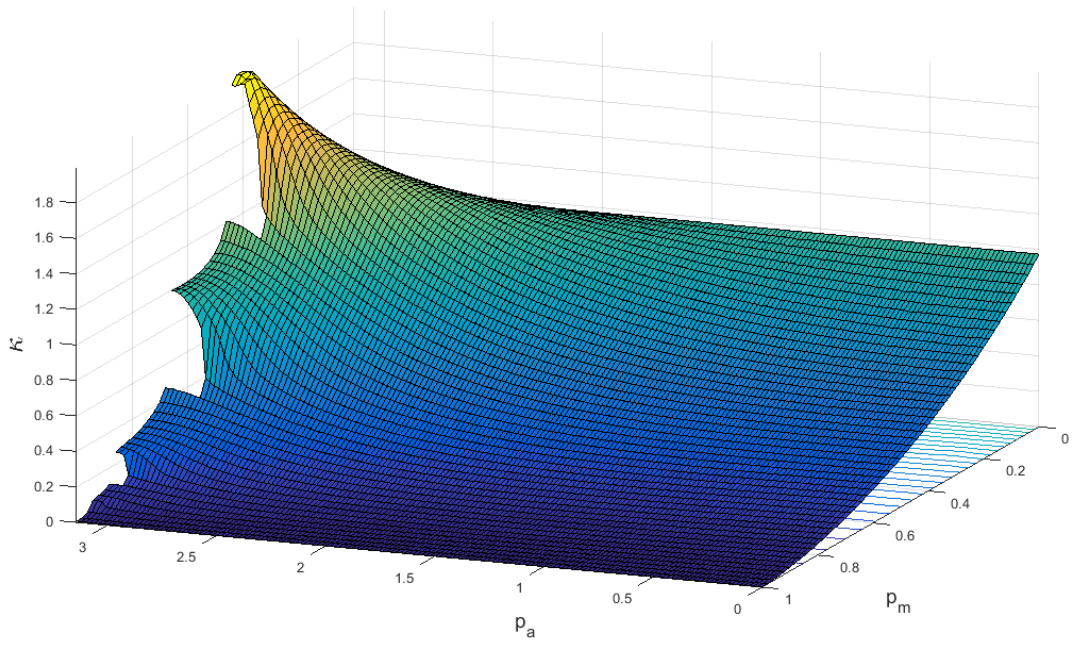

Figure 9: Critical manifold on the parameter space for the 987/1597-periodic orbit of the rational harmonic map (7), obtained by continuation over parameter κ for a regular grid on (p_a, p_m), starting from the integrable case $\kappa = 0$ and stopping for $|R| \sim 0.25$.

Following the spirit of the renormalization theory for symplectic maps, the critical manifold was computed for several rotation numbers F_{N-1}/F_N with N=11 (89/144), 18(2584/4181), 19(4181/6765), 20(67651/10946), following the same continuation as in for N=16 (987/1597) in Fig. 9. The apparent shape of the manifold remained unchanged, which shows the consistency between Greene's residue and renormalization theory. A more detailed comparison between the critical manifolds of these different rotation numbers can be appreciated in Figs. 11. The computational cost to compute the whole manifold for all the (p_a, p_m) domain increased significantly for greater periods and because of this reason the domain was reduced to $[0.4, 0.9] \times [0, \pi]$ with an equally spaced grid of step size of 0.02 and a maximum period of $F_{20} = 10946$.

It can be appreciated in Figs. 11 that the difference between critical values of κ between rotation numbers $F_{10}/F_{11} = 89/144$ and $F_{15}/F_{16} = 987/1597$ are of order 10^{-5}, while it is of order 10^{-6} between higher periods. This kind of experiments have not been done in the past for non-reversible maps or at least for maps without the use of symmetries.

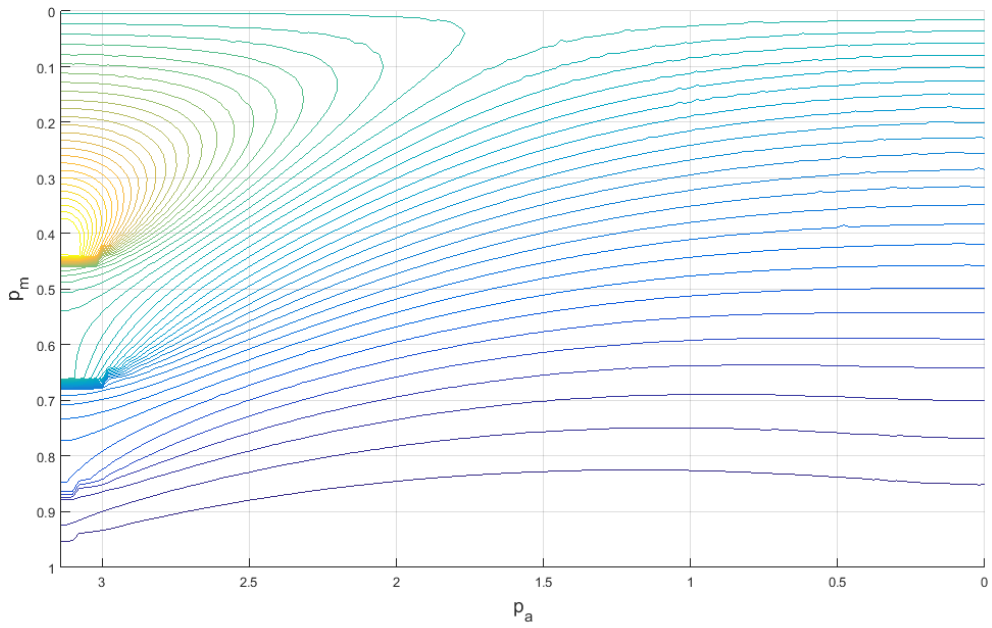

Figure 10: Level lines of the critical manifold from Fig. 9.

6.3 Beyond the break up in the *rational harmonic map*

A surprising benefit not originally considered in the implementation of this method, is that it is possible to continue the periodic orbits beyond the break up of the invariant circle. It is increasingly difficult for high order periodic orbits, but it is possible to compute them and obtain particular information about the *resurgence* of a given invariant circle. This *resurgence* can be easily understood if we consider that the continuation on parameter κ is done along vertical lines that eventually may cross through the folds of critical manifold. A different way to appreciate the *resurgence* can be seen in Fig. 12 in the κ-residue plane where for $(p_a, p_m) = (3.0, 0.4)$ the residue of five different F_{n-1}/F_n-periodic orbits beyond the Greene breaking re-collapse bellow $|R| \lesssim 0.25$ for $\kappa \in [1.41, 2.25]$, which implies the resurgence of the golden mean invariant circle.

7 Discussion

The method presented this work can be applied to a wide variety of maps to compute in a very efficient manner periodic orbits. There is no need to ask for symmetries to simplify or

$\frac{p}{q}$	Orbit x	E	R
$\frac{8}{13}$	$9.84400324333751592206 \times 10^{-01}$	1.5314×10^{-04}	-2.1690×10^{-01}
	$9.84194430418146115882 \times 10^{-01}$	4.8935×10^{-39}	-2.1777×10^{-01}
$\frac{21}{34}$	$9.97753743054888484767 \times 10^{-01}$	1.3827×10^{-05}	-1.8059×10^{-01}
	$9.97722363363172234098 \times 10^{-01}$	1.6284×10^{-47}	-1.8095×10^{-01}
$\frac{55}{89}$	$4.35066410514029663774 \times 10^{-04}$	2.8190×10^{-03}	-2.8817×10^{-01}
	$4.42076348408883988105 \times 10^{-04}$	1.8242×10^{-37}	-1.0589×10^{-01}
$\frac{144}{223}$	$4.09885888135278521212 \times 10^{-04}$	8.3211×10^{-11}	-1.3204×10^{-01}
	$4.54519288406945185848 \times 10^{-04}$	8.2324×10^{-29}	-2.5599×10^{-02}
$\frac{377}{610}$	$4.54770852734730605323 \times 10^{-04}$	8.6265×10^{-05}	-2.5479×10^{-02}
	$5.10890552501945729879 \times 10^{-04}$	1.2373×10^{-29}	-6.2363×10^{-04}
$\frac{987}{1597}$	$2.18102889348964055253 \times 10^{-04}$	9.4507×10^{-11}	-9.2787×10^{-08}
	$2.88969724223810721485 \times 10^{-04}$	9.5395×10^{-31}	-4.0099×10^{-08}
$\frac{2584}{4181}$	$5.70931653171076079438 \times 10^{-03}$	1.1379×10^{-24}	-3.2521×10^{-19}
	$5.70811191353601822914 \times 10^{-03}$	1.1872×10^{-31}	-3.2944×10^{-19}
$\frac{6765}{10946}$	$1.23693970334899424212053377 \times 10^{-02}$	3.1733×10^{-28}	-8.6237×10^{-24}
	$1.23693970334899424212053376 \times 10^{-02}$	9.5204×10^{-29}	-2.0985×10^{-24}

Table 3: Angular component x of the point closets to $x = 0$ of a few P/Q hyperbolic periodic orbits found for the *rational harmonic map* (7) with $(\kappa, p_a, p_m) = (1.7150, 3.0, 0.4)$, computed by the modified parameterization method (white rows) and then refined by a 2-D Newton method (gray rows) until $E < 10^{-28}$.

reduce the space of search. In the cases considered, the only requirement was that the maps were symplectic and additionally twist to justify some hypothesis from the parameterization method. The method as it is presented do not consider the case when the computed periodic orbits are close to a *meandering invariant circle*, see [10, 11]. In principle the method can be generalized to any other setup in which the standard parameterization method has been applied (see Ref. [21]), so an implementation for non-twist maps is not only possible but work in progress. It was found that the *modified parameterization method* (MPM) is efficient and very fast to find periodic orbits in cases where the parameters values are relatively close to the integrable case ($R \lesssim 10^{-8}$). And conversely, the Newton-Gauss method was found to be very efficient to find periodic orbits if with a data seed close to the critical parameter values ($R \gtrsim 10^{-8}$), although it is relatively slow as continuation method for parameter values farther of criticality. Both methods can be used to find periodic orbits but each one excel in complementing regimen. The compound method takes the strengths of each scheme and allows the computation of periodic orbits of high period in a relatively fast and efficient way.

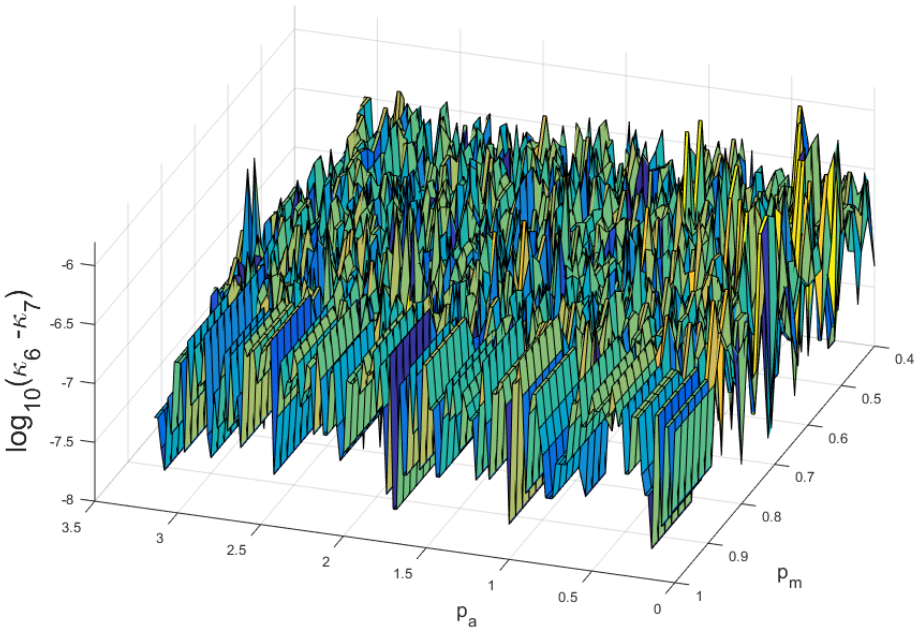

Figure 11: Absolute difference between two manifolds on the parameter space corresponding to: 4181/6765- and 67651/10946- periodic orbits of the rational harmonic map (7) obtained by continuation over parameter κ for a regular grid on (p_a, p_m), starting from the integrable case $\kappa = 0$ and stopping for $|R| \sim 0.2554$.

The application of the method to non-autonomous maps is possible for periodic cases as the one presented in Ref. [23]. The composition of q iterations of a given periodic non-autonomous twist map T of period q, generally yields a very convoluted map T^q that may not have obvious symmetries and in general there are regions in phase space where the map is not twist. The compound method does not have such requirements so it allows the computation of periodic orbits in a T^q map than later can be related to the original map. As described in Ref. [23], results from renormalization theory and just the computation of critical exponents only makes sense in the compound map. In the non-autonomous maps, the phase space is not two dimensional and the orbit is not well defined in the projection to the cylinder. The authors will present results for non autonomous periodic maps in a future publication.

The numerical experiments performed allowed to verify results from the renormalization theory in two different ways. First following the continuation of periodic orbits of rotation numbers (F_{N-1}/F_N) that approximate the *golden* invariant circle (of rotation number γ^{-1}), it was found an agreement between the critical residue value for both the standard map and

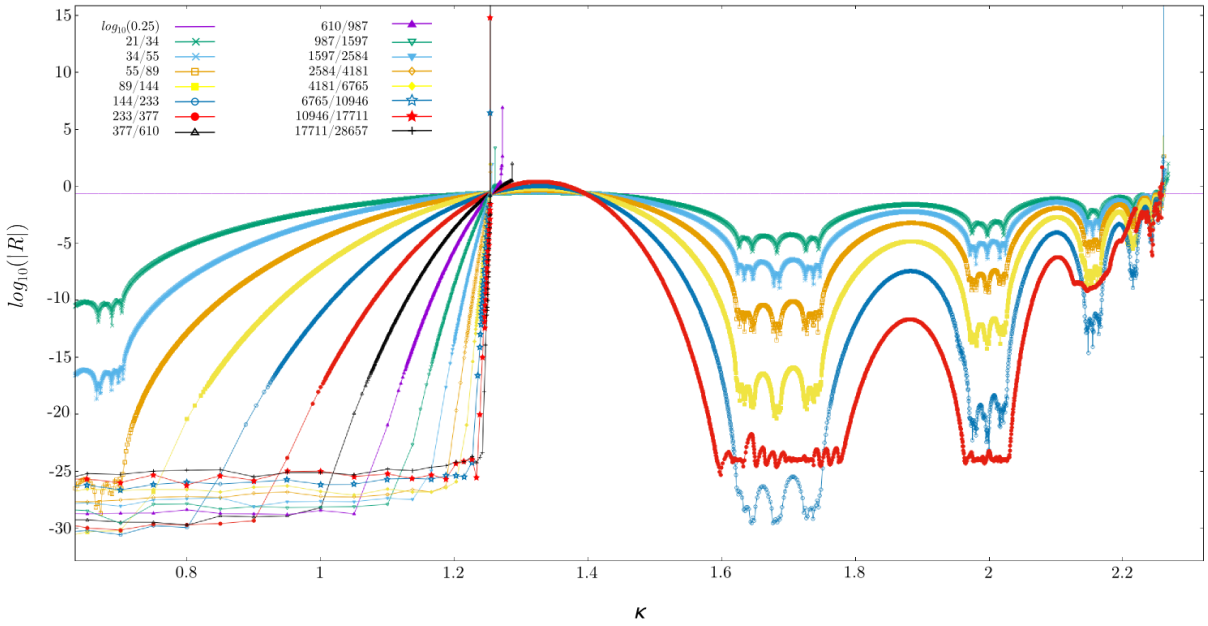

Figure 12: Residue of periodic orbits as function of the parameter κ in the rational harmonic map (7) for $(p_a, p_m) = (3.0, 0.4)$.

the *rational harmonic map* (figures 7 and 8). Additionally for the RHM it was observed a *resurgence* of golden invariant circle for an extended value of the parameter κ (Fig. 12). Secondly, to explore renormalization properties in the RHM for a wide range of parameters values, we performed a parameter sweep over a regular grid of (p_a, p_m) to associate them the value of κ corresponding to the case where the continued periodic orbit's absolute residue $|R|$ reached the critical residue value reported by Greene. The parameter sweep performed for several periodic orbits with Fibonacci's ratios as rotation numbers showed that the critical parameter value κ was almost the same for every (p_a, p_m) pair, as predicted by renormalization theory, see Figs. 9 - 11.

To the authors knowledge, a verification of renormalization theory for maps without symmetries as the case of RHM has not been performed in the past. The results show the consistency between Greene's residue conjecture and the universality of critical scalings predicted by renormalization theory. We believe that the use of Greene's residue criterion together with the continuation method we propose here, may help to determine when a broken invariant circle may reappear for larger values of the parameters after it has broken up.

The generalization of the method in this work to higher dimensions is limited only by the same restrictions of the parameterization method, easier implemented on even dimensions

and may require modifications for systems with small dissipation [49].

Applying the the Newton-Gauss method to higher dimensions seems to be plausible since the only restriction is that the size of the matrix $DG(\mathbf{z})$ and the number of operations will increase. We should emphasize that in both cases the increases will remain related to the order of the periodic orbit in an analogous manner to the 2-D case. The authors are working in the implementation of the method to maps of the Froeschlé type.

Acknowledgments

This work was founded by PAPIIT IN112920, IN110317, IA102818 and IN101020, FENOMEC-UNAM and by the Office of Fusion Energy Sciences of the US Department of Energy at Oak Ridge National Laboratory, managed by UT-Battelle, LLC, for the U.S.Department of Energy under contract DE-AC05-00OR22725. This material is based upon work supported by the National Science Foundation under Grant No. DMS-1440140 while R.C. and D.M. were in residence at the Mathematical Sciences Research Institute in Berkeley, California, during the Fall 2018 semester. We are indebted with À. Haro for sharing with us the ideas behind the implementation of the Newton-Gauss method. Also it is a pleasure to acknowledge the insightful discussions we had at Berkeley with J.D. Meiss, N. Petrov and A. Wurm. We also express our gratitude to the graduate program in Mathematics of UNAM for making the GPU servers available to perform our computations and especially to Ana Perez for her invaluable help.

References

[1] J.D. Meiss. Symplectic maps, variational principles, and transport. *Rev. Modern Phys.*, 64(3):795–848, 1992.

[2] B.V. Chirikov. A universal instability of many-dimensional oscillator systems. *Physics reports*, 52(5):263–379, 1979.

[3] J. M. Greene. A method for determining a stochastic transition. *Journal of Mathematical Physics*, 20:1183–1201, June 1979.

[4] L.P. Kadanoff. Scaling for a critical Kolmogorov-Arnold-Moser trajectory. *Physical Review Letters*, 47(23):1641, 1981.

[5] R.S. MacKay. *Renormalization in area-preserving Maps*. Disertation, Princeton University, 1982.

[6] S.J. Shenker and L.P. Kadanoff. Critical behavior of a KAM surface: I. empirical results. *Journal of Statistical Physics*, 27(4):631–656, 1982.

[7] R. DeVogelaere. Contributions to the theory of nonlinear oscillations, edited by S. Lefschetz (Princeton UP, Princeton, NJ, 1958), Vol. IV.

[8] J. B. Taylor. Unpublished. 1969.

[9] A.J. Lichtenberg and M.A. Lieberman. *Regular and chaotic dynamics*, volume 38. Springer Science & Business Media, 2013.

[10] D. del-Castillo-Negrete. *Dynamics and Transport in Rotating Fluids and Transition to Chaos in Area Preserving Non-twist Maps*. PhD thesis, PhD Thesis, Univ. of Texas, Austin, 1994.

[11] K. Fuchss, A. Wurm, A. Apte, and P.J. Morrison. Breakup of shearless meanders and "outer" tori in the standard nontwist map. *Chaos*, 16(3):033120, 2006.

[12] D. del-Castillo-Negrete, J.M. Greene, and P.J. Morrison. Area preserving nontwist maps: periodic orbits and transition to chaos. *Physica D: Nonlinear Phenomena*, 91(1):1–23, 1996.

[13] D. del-Castillo-Negrete, J.M. Greene, and P.J. Morrison. Renormalization and transition to chaos in area preserving nontwist maps. *Physica D: Nonlinear Phenomena*, 100(3-4):311–329, 1997.

[14] A. Apte, R. de la Llave, and N.P. Petrov. Regularity of critical invariant circles of the standard nontwist map. *Nonlinearity*, 18(3):1173–1187, 2005.

[15] A. González-Enríquez, À. Haro, and R. De la Llave. *Singularity theory for non-twist KAM tori*, volume 227. Memoirs of the American Mathematical Society, 2014.

[16] H. Kook and J.D. Meiss. Periodic orbits for reversible, symplectic mappings. *Physica D: Nonlinear Phenomena*, 35(1-2):65–86, 1989.

[17] A. Olvera and C. Vargas. A continuation method to study periodic orbits of the Froeschlé map. *Physica D: Nonlinear Phenomena*, 72(4):351–371, 1994.

[18] R. Calleja and R. de la Llave. Fast numerical computation of quasi-periodic equilibrium states in 1D statistical mechanics, including twist maps. *Nonlinearity*, 22(6):1311–1336, 2009.

[19] R. Calleja and R. de la Llave. Computation of the breakdown of analyticity in statistical mechanics models: numerical results and a renormalization group explanation. *J. Stat. Phys.*, 141(6):940–951, 2010.

[20] R. de la Llave, A. González, À. Jorba, and J. Villanueva. KAM theory without action-angle variables. *Nonlinearity*, 18(2):855–895, 2005.

[21] À. Haro, M. Canadell, J.-Ll. Figueras, A. Luque, and J.-M. Mondelo. *The parameterization method for invariant manifolds. From rigorous results to effective computations.* Springer, 2016.

[22] D. Martínez-del-Río, D. del-Castillo-Negrete, A. Olvera, and R.C. Calleja. Self-consistent chaotic transport in a high dimensional mean-field hamiltonian map model. *QTDS*, 14(2):313–335, 2015.

[23] R. Calleja, D. del-Castillo-Negrete, D. Martínez-del-Río, and A. Olvera. Global transport in a nonautonomous periodic standard map. *Communications in Nonlinear Science and Numerical Simulation*, 51:198–215, 2017.

[24] R. Calleja and R. de la Llave. A numerically accessible criterion for the breakdown of quasi-periodic solutions and its rigorous justification. *Nonlinearity*, 23(9):2029–2058, 2010.

[25] L. Reichl. *The transition to chaos: conservative classical systems and quantum manifestations.* Springer Science & Business Media, 2013.

[26] D. Martinez-del Rio. *Study of the self-comnsistent chaotic transport throught a mean-field coupled dynamical system.* Disertation, UNAM, Mexico, 2019.

[27] R.L. Devaney. Reversible diffeomorphisms and flows. *Transactions of the American Mathematical Society*, 218:89–113, 1976.

[28] M.B. Sevryuk. Reversible systems. volume 1211 of lecture notes in mathematics, 1986.

[29] John A.G. Roberts and M.l Baake. Trace maps as 3d reversible dynamical systems with an invariant. *Journal of Statistical Physics*, 74(3):829–888, 1994.

[30] E. Piña and L. Jiménez-Lara. On the symmetry lines of the standard mapping. *Physica D: Nonlinear Phenomena*, 26(1-3):369–378, 1987.

[31] J.A.G. Roberts and G.R.W. Quispel. Chaos and time-reversal symmetry. order and chaos in reversible dynamical systems. *Physics Reports*, 216(2-3):63–177, 1992.

[32] A. Olvera and N. P. Petrov. Regularity properties of critical invariant circles of twist maps, and their universality. *SIAM Journal on Applied Dynamical Systems*, 7(3):962–987, 2008.

[33] J.E. Dennis Jr and R.B. Schnabel. *Numerical methods for unconstrained optimization and nonlinear equations*, volume 16. SIAM, 1996.

[34] H. Kook and J.D. Meiss. Application of newton's method to lagrangian mappings. *Physica D: Nonlinear Phenomena*, 36(3):317–326, 1989.

[35] Y.-G. Shi and L. Chen. Reversible maps and their symmetry lines. *Communications in Nonlinear Science and Numerical Simulation*, 16(1):363–371, 2011.

[36] A. Olvera and C. Simó. Private communication. 1987.

[37] A.M. Fox and J.D. Meiss. Critical invariant circles in asymmetric and multiharmonic generalized standard maps. *Commun Nonlinear Sci Numer Simulat*, 19(4):1004–1026, 2014.

[38] E. Zehnder. Generalized implicit function theorems with applications to some small divisor problems. I. *Comm. Pure Appl. Math.*, 28:91–140, 1975.

[39] G. Huguet, R. de la Llave, and Y. Sire. Computation of whiskered invariant tori and their associated manifolds: new fast algorithms. *Discrete Contin. Dyn. Syst.*, 32(4):1309–1353, 2012.

[40] J.-Ll. Figueras, À. Haro, and A. Luque. Rigorous computer assisted application of KAM theory: a modern approach. *ArXiv e-prints*, January 2016.

[41] À. Haro, M. Canadell, J.-Ll. Figueras, A. Luque, and J.-M. Mondelo. *The parameterization method for invariant manifolds. From rigorous results to effective computations.* Springer, 2016.

[42] R. Calleja and A. Celletti. Breakdown of invariant attractors for the dissipative standard map. *Chaos*, 20(1):013121, 9, 2010.

[43] R. Calleja and J.-Ll. Figueras. Collision of invariant bundles of quasi-periodic attractors in the dissipative standard map. *Chaos*, 22(3):033114, 10, 2012.

[44] A. M. Fox and J. D. Meiss. Greene's residue criterion for the breakup of invariant tori of volume-preserving maps. *Phys. D*, 243:45–63, 2013.

[45] A. Hungria, J.-P. Lessard, and J.D. Mireles-James. Rigorous numerics for analytic solutions of differential equations: the radii polynomial approach. *Mathematics of Computation*, 85(299):1427–1459, 2016.

[46] R. Castelli, J.-P. Lessard, and J.D. Mireles-James. Parameterization of invariant manifolds for periodic orbits (ii): A posteriori analysis and computer assisted error bounds. *Journal of Dynamics and Differential Equations*, pages 1–57, 2017.

[47] J. Burgos-García, J.-P. Lessard, and J.D. Mireles. Spatial periodic orbits in the equilateral circular restricted four-body problem: computer-assisted proofs of existence. *Celestial Mechanics and Dynamical Astronomy*, 131(1):2, 2019.

[48] J.-Ll. Figueras and À. Haro. Different scenarios for hyperbolicity breakdown in quasiperiodic area preserving twist maps. *Chaos*, 25(12):123119, 2015.

[49] R. Calleja, A. Celletti, and R. de la Llave. A KAM theory for conformally symplectic systems: efficient algorithms and their validation. *J. Differential Equations*, 255(5):978–1049, 2013.